Table 1. Nucleotide sequences of the polymerase chain reaction (PCR) primers, the expected sizes of the amplified products, annealing temperature, and cycle numbers of PCR reactions

Primers			Product	Annealing temperature	Cycles
RMCP II	5′ primer	5′-ACGAAAGTTACAACTCCGTTC-3′	475 bp	60°C	32
	3′ primer	5′-GTGTCTCAAGCAGGTCAGG-3′			
RMCP V	5′ primer	5′-GTCTATAACCGTCCTCCTAG-3′	381 bp	54°C	38
	3′ primer	5′-TTTTGCATCTTCTTGGGGTTG-3′			
RMCP VIII	5′ primer	5′-GGCCATCCTACCAGTCAACAC-3′	341 bp	60°C	30
	3′ primer	5′-CACCATTGAGTTGAGCTTTGCG-3′			
GAPDH	5′ primer	5′-GGGAGCCAAAAGGGTCATCATCTC-3′	516 bp	64°C	18
	3′ primer	5′-CCATGCCAGTGAGCTTCCCGTTC-3′			

All of the PCR reactions were performed as described in the **Methods** section.

Collection of Cell Cultures (Salisbury, UK) and maintained in Dulbecco's modified Eagle's medium (Invitrogen, Grand Island, NY, USA) supplemented with 10% fetal calf serum (FCS), glutamine, and nonessential amino acid equilibrated with 5% CO_2-95% air at 37°C. For experiments, cells grown to 80% confluence in 100-mm dishes were exposed to fresh medium with or without 100 μg/mL heparin (sodium salt; Sigma) for 6 hours and then used for RNA preparation.

Reverse transcription-polymerase chain reaction (RT-PCR)

Total RNA fractions were prepared from pieces of renal cortex or cultured cells by the guanidinium thiocyanate-phenol-chloroform method [27], and 5 μg of RNA was reverse-transcribed by use of oligo(dT) primers in 20 μL of buffer as previously described [28]. For the analysis of levels of mRNA for RMCPs II, V, and VIII, 1 μL of this reaction mixture containing the cDNA was amplified by PCR in 50 μL of 10 mmol/L Tris-HCl (pH 9.0) containing 50 mmol/L KCl, 1.5 mmol/L $MgCl_2$, 5′ and 3′ primers (Table 1), and Taq DNA polymerase (Promega, Madison, WI, USA). Aliquots were electrophoresed on a 2% agarose gel and visualized with ethidium bromide under ultraviolet illumination. For the quantitative measurement of cytokine mRNA levels, real-time PCR was performed by using an ABI PRISM 7700 Sequence Detector and TaqMan® Pre-Developed Assay Reagents for Gene Expression Quantification System (Applied Biosystems, Foster City, CA, USA). Using multiple reporter dyes, we assayed the mRNA levels of each cytokine and endogenous control (GAPDH) in the same tube and expressed cytokine mRNA levels as the ratio relative to the endogenous control.

Hydroxyproline analysis

The amount of hydroxyproline in the renal cortex was measured according to Kivirikko et al [29] as an index of collagen content. At sacrifice, pieces of renal cortex for the hydroxyproline assay were weighed, snap-frozen in liquid nitrogen, and stored at −80°C for subsequent use. The samples were hydrolyzed in 1 mL of 6N hydrochloric acid at 110°C for 18 hours in tightly capped tubes. After the hydrolysates had been neutralized with sodium hydroxide, their hydroxyproline content was assessed colorimetrically at 560 nm with *p*-dimethylaminobenzaldehyde. Results were expressed as ng per mg wet renal cortex.

Statistical analysis

All values were expressed as the mean ± SD. Data were analyzed by the Mann-Whitney *U* test, and a difference with a value of $P < 0.05$ was considered to be statistically significant.

RESULTS

PAN nephrosis in *Ws/Ws* and +/+ rats

In PAN nephrosis model induced by uninephrectomy and subsequent administration of PAN, increases in urinary protein excretion and BUN level were observed in both mast cell–deficient *Ws/Ws* and their control (+/+) littermates; there was no difference in either parameter between the two groups (Fig. 1). At 6 weeks, the level of urinary protein excretion markedly decreased because of the loss of functioning nephrons (end-stage renal failure).

Renal fibrosis induced in *Ws/Ws* and +/+ rats by PAN

Interstitial fibrosis occurred in both PAN-treated *Ws/Ws* and +/+ rats at 2 weeks at the border of the cortex-medulla. A significant expansion of the fibrotic area was observed at 6 weeks in both strains. Unexpectedly however, the fibrosis was more severe in the *Ws/Ws* rats than in their +/+ littermates (Fig. 2). No obvious fibrosis was observed in the control animals. The magnitude of fibrosis was semiquantitatively determined with light microscopy (Fig. 3). The degree of fibrosis was similar in both groups at 2 weeks, but was greater in *Ws/Ws* rats than in +/+ rats at 6 weeks.

To confirm these histologic results, we measured the hydroxyproline content in the renal cortex (Fig. 4). At 2 weeks, although the content of this collagen marker

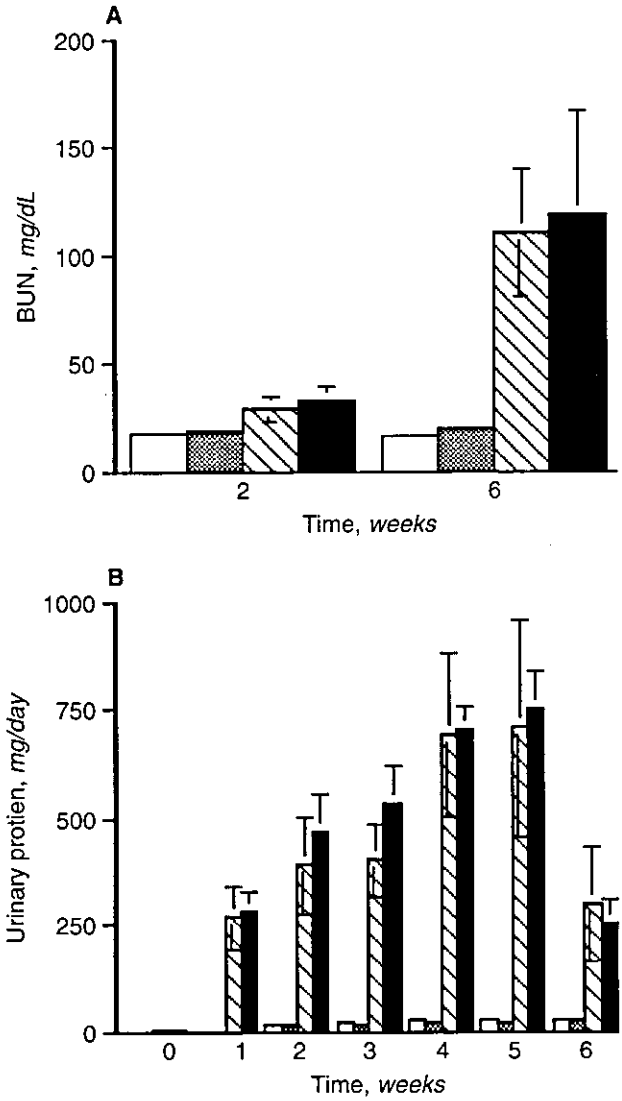

Fig. 1. Clinical course of puromycin aminonucleoside (PAN) nephrosis in *Ws/Ws* and +/+ rats. Blood urea nitrogen (*A*), urinary protein excretion (*B*). Control +/+ (□); Control *Ws/Ws* (■); PAN-treated +/+ (⊡); PAN-treated *Ws/Ws* rats (■).

in PAN-treated animals was slightly higher than that in control animals, the difference was not statistically significant; and the level was similar in PAN-treated *Ws/Ws* and +/+ rats. At 6 weeks, the content was significantly greater in PAN-treated animals than in control animals. Moreover, the level in the PAN-treated *Ws/Ws* rats was significantly higher than that in the PAN-treated +/+ rats. Thus, the fibrotic changes in the interstitium assessed by both histologic and biochemical methods were greater in *Ws/Ws* rats than in their +/+ littermates.

Interstitial mast cells in PAN-induced nephrosis

Mast cells were immunohistochemically identified by their immunoreactivity, indicating the presence of RMCP I, a specific marker for mast cells [30, 31]. An almost complete absence of mast cells in the skin of *Ws/Ws* rats was confirmed by immunostaining for RMCP I (data not shown). Practically no mast cells were detectable in the kidney of control *Ws/Ws* and +/+ rats. However, in the kidney tissues of PAN-treated +/+ rats, mast cells were observed in the interstitium, where they showed a scattered distribution (Fig. 5A). Most were localized in the peritubular region (Fig. 5B).

To confirm the increase in the number of mast cells in the kidney, we also examined mRNA levels of other specific markers for mast cells (i.e., RMCPs II, V, and VIII). By RT-PCR analysis, mRNAs for all of these proteases were consistently found in disease-induced rats, but not in control rats, by the experimental procedures used (Fig. 6).

The time-kinetics of the number of interstitial mast cells determined by immunohistochemistry is illustrated in Figure 7. After administration of PAN, the number of mast cells increased significantly in both *Ws/Ws* and +/+ rats, but was lower in the former than in the latter. While the number of mast cells gradually increased in PAN-treated +/+ rats with the expansion of the interstitial fibrosis, the number in PAN-treated *Ws/Ws* rats decreased with the continued expansion. The number in PAN-treated *Ws/Ws* rats was one half at 2 weeks and one fifth at 6 weeks compared with that in the PAN-treated +/+ rats.

Other interstitial cells in PAN-induced nephrosis

Because thymocytes are *c-kit*–positive cells, the defect in *c-kit* carried by *Ws/Ws* rats could potentially affect T-cell development, although there have been no reports showing such T-cell deficits. It is also known that myofibroblasts express *c-kit* [32]. To clarify the influence of the *c-kit* deletion in these types of cell in the kidney of *Ws/Ws* rats, we examined the levels of monocytes/macrophages, CD4–, CD8–, and α–SMA–positive cells in the interstitium (Table 2). Low numbers of these types of cells were detected in the interstitium of the control animals. After the disease induction, their numbers increased in both *Ws/Ws* and +/+ rats, but there were no differences in them between the two strains. Most of the monocyte/macrophages and CD4– and CD8– positive cells were found in the interstitial lesion in clusters, especially in the area around glomeruli and disrupted tubuli, and the localization was different from that of the mast cells.

Cytokine mRNA levels in renal cortex

To investigate the possible mechanism for the increase in fibrosis in these *Ws/Ws* rats, we measured mRNA levels of cytokines that might affect the progression of fibrosis. As shown in Figure 8, the levels of mRNA for two potentially profibrotic cytokines, TGF-β and interleukin (IL)-4,

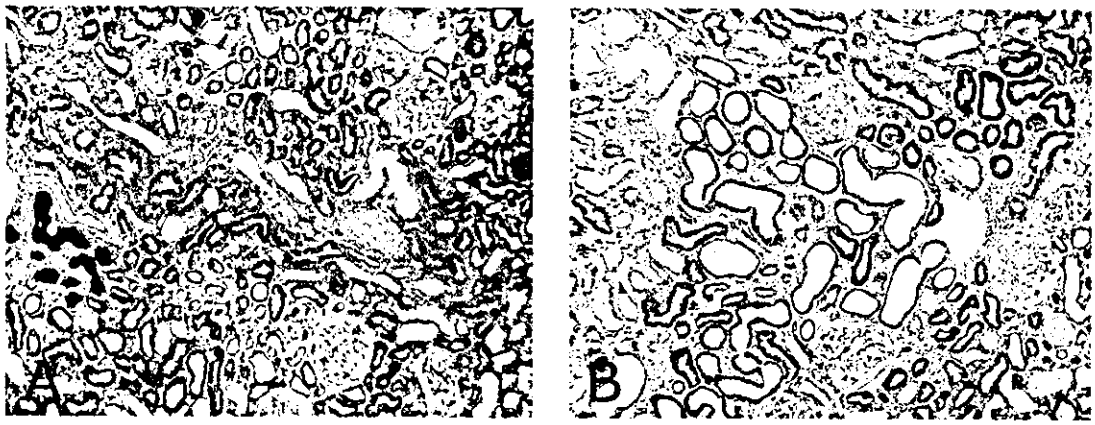

Fig. 2. Representative histologic changes in the kidney in puromycin aminonucleoside (PAN) nephrosis. Kidney tissues were obtained at 6 weeks from PAN-treated +/+ rats (*A*) and PAN-treated *Ws/Ws* rats (*B*). Masson-trichrome staining. Original magnification ×100.

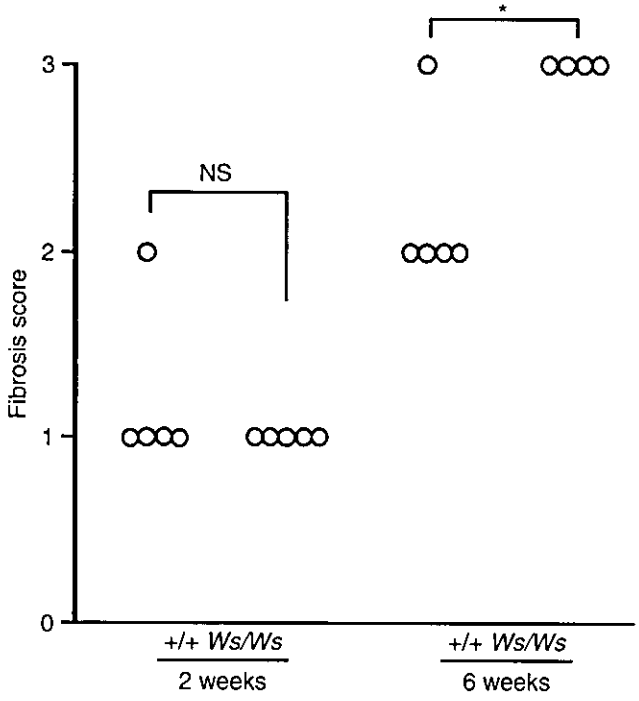

Fig. 3. Semiquantification of the fibrotic interstitium in puromycin aminonucleoside (PAN) nephrosis. Kidney tissues were obtained at 2 and 6 weeks from PAN-treated +/+ and *Ws/Ws* rats. $^{*}P < 0.05$.

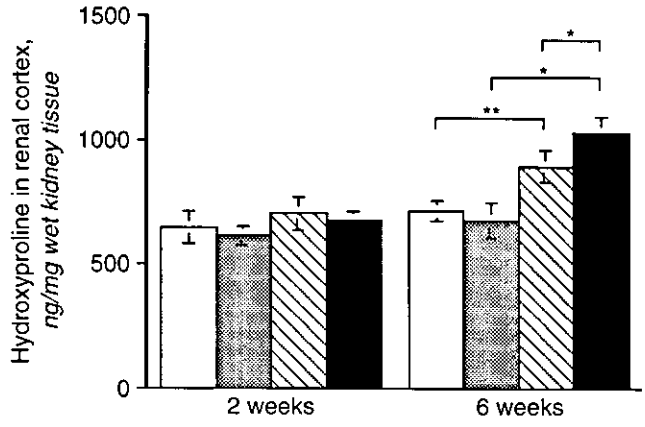

Fig. 4. Hydroxyproline content in renal cortex of rats with puromycin aminonucleoside (PAN) nephrosis. Control +/+ (□); control *Ws/Ws* (■); PAN-treated +/+ (▨); PAN-treated *Ws/Ws* rats (■). $^{*}P < 0.05$; $^{**}P < 0.01$.

were higher in the *Ws/Ws* rats than in the +/+ ones. The differences between the two groups in the level of TGF-β mRNA at 2 weeks, and in that of IL-4 mRNA at 6 weeks, were statistically significant. There were no differences in mRNA levels of IL-2, IL-10, and interferon (IFN)-γ in the renal cortex between the two strains. These results suggest that the enhanced production of TGF-β and/or IL-4 in *Ws/Ws* rats may have caused the enhanced fibrosis in the kidney.

Effect of heparin on the expression of TGF-β1 mRNA in renal fibroblast in culture

Although mast cells have been shown to produce TGF-β and IL-4 in culture [9], they also produce other cytokines and factors that may modulate the production of these cytokines by other types of cells. Heparin is a major component stored in secretory granules of mast cells and is known to influence cytokine production in culture [33]. Therefore, using a cell line of interstitial fibroblasts derived from normal rat kidney, we investigated if heparin could influence the production of TGF-β in culture. As shown in Figure 9, the expression of TGF-β mRNA in renal fibroblast was inhibited by heparin.

DISCUSSION

In progressive human glomerular diseases, regardless of their type, the number of interstitial mast cells

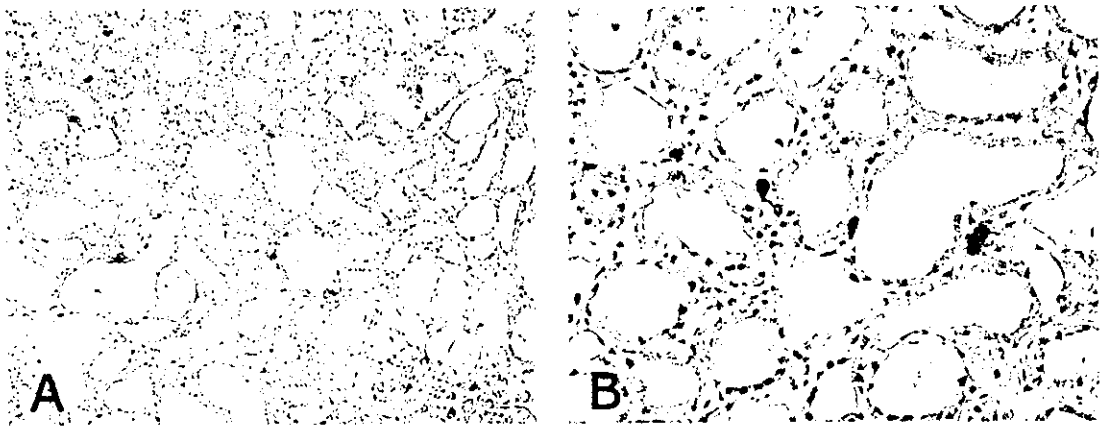

Fig. 5. Immunostaining for rat mast cell protease (RMCP) I, a specific marker for mast cell, in puromycin aminonucleoside (PAN) nephrosis. Representative kidney sections obtained at 6 weeks from PAN-treated +/+ rats are shown. RMCP I-positive cells with a scattered distribution are seen in the interstitium (*A*). These cells are mostly located in the peritubular region (*B*). Original magnification, ×100 (A) and ×200 (B).

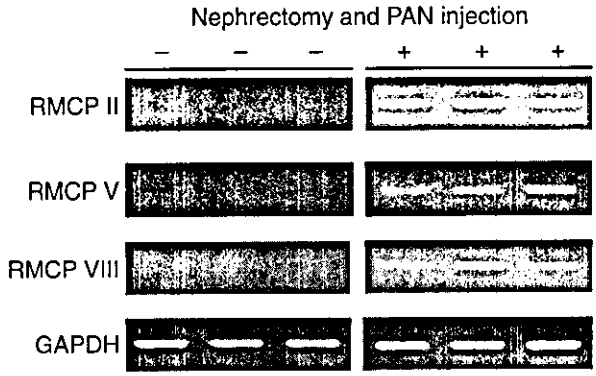

Fig. 6. Expression of mRNA for rat mast cell proteases (RMCPs) II, V, and VIII. RNA extracted from 3 animals of each group [2-week puromycin aminonucleoside (PAN)-treated +/+ rats and control +/+ rats] was used for reverse transcription-polymerase chain reaction (RT-PCR) analysis. Each lane represents the mRNA expression of each animal. The GAPDH band is shown as the internal control.

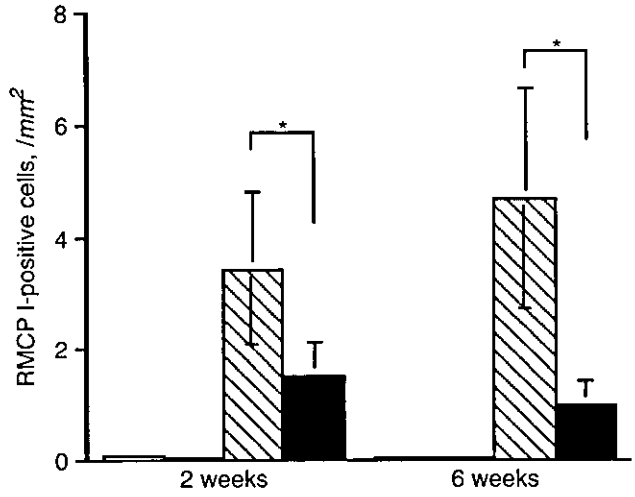

Fig. 7. Numbers of interstitial rat mast cell protease (RMCP) I-positive cells in puromycin aminonucleoside (PAN) nephrosis. Control +/+ (□); control *Ws/Ws* (■); PAN-treated +/+ (▨); PAN-treated *Ws/Ws* rats (■). $^*P < 0.05$.

increases as interstitial fibrosis expands [14, 15, 17]. The present study has demonstrated that in PAN nephrosis, a rat model of progressive glomerular disease, the number of interstitial mast cells also increased concomitant with the expansion of interstitial fibrosis. We also found that the number of interstitial mast cells increased in the crescentic glomerulonephritis model in Wistar Kyoto rats (our unpublished observations). These results indicate that, like in humans, mast cells accumulate in the interstitial area in progressive renal diseases in rats when interstitial fibrosis develops.

Because PAN nephrosis can be induced in any strain of rat, using mast cell–deficient *Ws/Ws* rats, we then investigated the suggested causal link between mast cell accumulation and interstitial fibrosis. Unexpectedly, interstitial fibrosis was markedly worse in these rats. Although mast cells were not completely absent in the diseased kidney of *Ws/Ws* rats, their number at 6 weeks in PAN-treated *Ws/Ws* rats was approximately one fifth of that in the PAN-treated control littermates. Because it was shown that the number of mast cells in the whole body of *Ws/Ws* rats is decreased by aging [23], we considered that the decrease in the number of interstitial mast cells from 2 to 6 weeks in the rats resulted from aging and is irrelevant to the development of interstitial fibrosis. The observed interstitial mast cells in the *Ws/Ws* rats may have resulted from the accumulation of the remaining small number of mast cells from other parts of the body [34]. In contrast, there were no differences between the two strains in the levels of interstitial T lymphocytes and myofibroblasts, two types of cell that could be affected by the *c-kit* gene mutation in *Ws/Ws* rats. Taken together, these results suggest that the reduction in the number of interstitial mast cells in *Ws/Ws* rats resulted in the exacerbation of interstitial fibrosis in this model.

Table 2. Interstitial cells in +/+ and *Ws/Ws* rats at 6 weeks

	Control		PAN nephrosis	
	+/+	*Ws/Ws*	+/+	*Ws/Ws*
ED-1 (monocytes/macrophages)[a]	83.8 ± 13.3	80.0 ± 10.6	570.0 ± 40.1	592.0 ± 46.3
W3/25 ($CD4^+$ cells)[a]	157.4 ± 14.4	165.8 ± 11.8	593.9 ± 42.4	580.0 ± 36.0
OX8 ($CD8^+$ cells)[a]	21.1 ± 10.3	16.6 ± 4.8	116.5 ± 12.7	112.8 ± 12.6
α-SMA (myofibroblast)[b]	1.2 ± 0.3	1.3 ± 0.3	11.6 ± 1.1	10.5 ± 3.3

α-SMA, alpha-smooth muscle actin.
[a]Data are the numbers of interstitial cells per mm^2 expressed as mean ± SD ($N = 5$).
[b]Data are % interstitial positive area expressed as mean ± SD ($N = 5$).

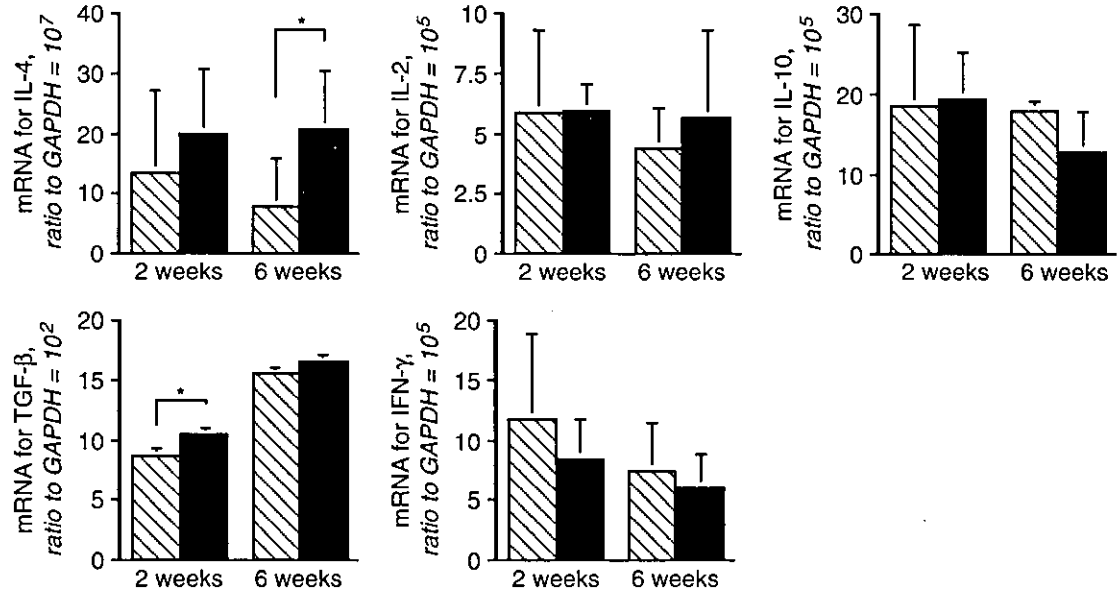

Fig. 8. Expression of cytokine mRNA levels in renal cortex of rats with puromycin aminonucleoside (PAN) nephrosis. Data are expressed as the ratio to the internal control. PAN-treated +/+ (□); PAN-treated *Ws/Ws* rats (■). $^*P < 0.05$.

It was demonstrated earlier that myofibroblast proliferation is paralleled by or precedes the development of interstitial fibrosis in human and animal models [35], but the result of the present study is not consistent with those previous studies. It could be possible that there is some unknown effect that originated from the mutated *c-kit* gene that changed the functions of myofibroblasts in *Ws/Ws* rats. In addition, we cannot exclude the possibility that the mutated *c-kit* gene causes other abnormalities than mast cell deficiency, although there have been no reports so far that show such defects in *Ws/Ws* rats except for anemia in their early life [23].

Our present study using mast cell–deficient *Ws/Ws* is the first one to our knowledge to reveal the role of mast cells in renal fibrosis. There have been some earlier studies in which the involvement of mast cells in fibrosis of lung [36, 37], liver [36, 38], and skin [39, 40] was examined by using mast cell–deficient W/W^v mice and/or *Ws/Ws* rats. Some of these studies showed no difference in the magnitude of fibrosis between the mast cell–deficient animals and their control +/+ littermates, which suggested that mast cells do not appear to be necessary for the induction of fibrosis. In the present study, our histologic and biochemical analysis revealed that the fibrosis was more severe in *Ws/Ws* rats than in +/+ littermates at 6 weeks after the induction of PAN nephrosis. These data are consistent with other studies on lung [36, 37] and liver [36] fibrosis, which showed that the increase in the hydroxyproline content of the tissues of deficient animals was greater than that in control +/+ littermates.

The mechanism by which greater renal interstitial fibrosis occurred in *Ws/Ws* rats with PAN nephrosis is unclear. We investigated the possibility that levels of cytokines that potentially enhance directly or indirectly the progression of fibrosis are changed in *Ws/Ws* rats with PAN nephrosis. The cytokines tested in this study included Th1 and Th2 cytokines, the balance of which is suggested to affect fibrotic changes [41]. Our results showed that mRNA levels of TGF-β and IL-4 were higher in *Ws/Ws* rats than in controls in the PAN nephrosis model,

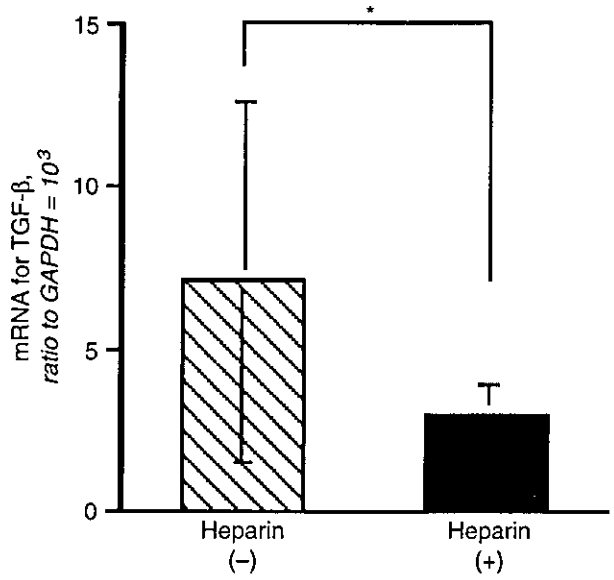

Fig. 9. Inhibition of expression of transforming growth factor (TGF)-β1 mRNA by heparin. Rat renal fibroblasts were cultured in the absence (□) or presence (■) of heparin for 6 hours. Data are expressed as mean ± SD of 5 samples.

suggesting that the deficiency of mast cells (i.e., in *Ws/Ws* rats) may have caused an increase in their expression, resulting in more fibrosis in the *Ws/Ws* rats.

Mast cells contain a variety of mediators that have been shown to directly or indirectly affect the progression of fibrosis in tissues [42]. Although mast cells have been shown to produce TGF-β and IL-4 in culture [9], they also produce other cytokines and factors that may modulate cytokine production by other types of cells. Heparin, a major component stored in secretory granules of mast cells, was shown to have effects on cell proliferation [43] and cytokine production [33], both of which are involved in the pathogenesis of fibrosis. Heparin was also shown to inhibit DNA synthesis by human renal fibroblasts when added alone, although it enhanced DNA synthesis when added with tryptase, a proteolytic enzyme secreted by mast cells [44]. The present study demonstrated that heparin inhibited the gene expression of TGF-β, the most potent fibrogenic cytokine, in renal fibroblasts in culture. A recent study also demonstrated that heparin inhibited the production of TGF-β by cultured human proximal tubular epithelial cells, another source of the cytokine in diseased kidney [45]. Therefore, it is conceivable that heparin secreted from mast cells may inhibit TGF-β production by these cells in the diseased kidney and that this action may have contributed to the less fibrosis in the control +/+ littermates in the PAN nephrosis model. We also tested the effect of heparin on IL-4 production by these cells, but the production level was very low, and thus the effect of heparin could not be detected (our unpublished observation).

The results of the present study using mast cell–deficient animals seem to be in conflict with a suggested role of mast cells in renal diseases. The profibrogenic role of mast cells has been proposed mostly based on histologic observations of clinical samples and results of in vitro studies using cultured cells [14–20, 44]. However, the histologic studies only showed a correlation between the two phenomena, mast cell accumulation and fibrosis, and do not provide evidence of a causal link between them. In vitro studies, on the other hand, give data on the potential effects of mast cells or their secretory components on fibrosis, but do not provide information about the overall effect of mast cells. Even if whole components stored in mast cells or mast cells themselves are used in a culture system, one cannot provide all cells and extracellular circumstances of the kidney in the in vitro system. Further studies are needed to elucidate the role of mast cells in the mechanism of fibrosis, but we consider that experiments using animal models as well as intervention studies in humans will be necessary to assess the effect of mast cells as a whole on fibrosis.

In the kidney of the animal models of glomerular diseases we tested, mast cells were localized in a scattered distribution in the interstitium, whereas interstitial mononuclear cells (MNC), mostly consisting of monocytes/macrophages and T lymphocytes, were present in clusters. In human glomerular diseases on the other hand, mast cells were restricted to the area of interstitial fibrosis where only a few T lymphocytes and macrophages were concomitantly present, but were rarely found in the interstitial lesion where the influx of MNC was pronounced (our unpublished observations). This interstitial influx of MNC presumably precedes the interstitial fibrosis and is suggested to be involved in the mechanism of fibrotic changes [46]. Therefore, in consideration of these findings, together with the results of the present study, it is conceivable that mast cells are not involved in the development of fibrosis because of their absence in prefibrotic lesions in contrast to T lymphocytes or macrophages, but are attracted in fibrotic lesion and possibly participate in the attenuation or resolution of the fibrotic lesions. Unfortunately, in the rodent models it was rather difficult to discriminate prefibrotic lesions from established areas of fibrosis, probably because of the short duration and/or acute inflammation after the disease onset.

CONCLUSION

In the present study, we investigated the role of mast cells in the development of renal fibrosis by using mast cell–deficient rats. In human studies, mast cells are thought to be one of the cell types contributing to the interstitial fibrosis. However, it could be mentioned from our data that mast cells are not simply fibrogenic. Rather, they might have a potential to be protective or

ameliorative in this model and possibly in other models and also in humans.

ACKNOWLEDGMENTS

We are grateful to Dr. Takashi Oda, National Defense Medical College, for his advice concerning the hydroxyproline analysis. This work was supported in part by a Health Science Research Grant (Research on Specific Diseases) from the Ministry of Health and Welfare. Portions of this work were presented at the 2001 Annual Meeting of the American Society of Nephrology and reported in abstract form (*J Am Soc Nephrol* 12:711A, 2001).

Reprint requests to Dr. Yasuhiro Natori, Department of Clinical Pharmacology, Research Institute, International Medical Center of Japan, Toyama 1-21-1, Shinjuku-ku, Tokyo 162-8655, Japan.
E-mail: natoriya@ri.imcj.go.jp

REFERENCES

1. Pesci A, Bertorelli G, Gabrielli M: Mast cells in fibrotic lung disorders. *Chest* 103:989–996, 1993
2. Pesci A, Majori M, Piccili ML, *et al*: Mast cells in bronchiolitis obliterans organizing pneumonia: Mast cell hyperplasia and evidence for extracellular release of tryptase. *Chest* 110:383–391, 1996
3. Murata K, Okudaira M, Akashio K: Mast cells in human liver tissue. Increased mast cell number in relation to the components of connective tissue in the cirrhotic process. *Acta Derm Venereol* 73:157–165, 1973
4. Armbrust T, Batusic D, Ringe B, *et al*: Mast cell distribution in human liver disease and experimental rat liver fibrosis: Indications for mast cell participation in development of liver fibrosis. *J Hepatol* 26:1042–1054, 1997
5. Hawkins RA, Claman HN, Clark RAF, *et al*: Increased dermal mast cell populations in progressive systemic sclerosis: A link in chronic fibrosis? *Ann Intern Med* 102:182–186, 1985
6. Rothe MJ, Nowak M, Kerdel FA: The mast cell in health and disease. *J Am Acad Dermatol* 23:615–624, 1990
7. Craig SS, DeBlois G, Schwartz LB: Mast cells in human keloid, small intestine, and lung by an immunoperoxidase technique using a murine monoclonal antibody against tryptase. *Am J Pathol* 124:427–435, 1986
8. Schwartz LB: Mast cells: Function and contents. *Curr Opin Immunol* 6:91–97, 1994
9. Gordon JR, Burd PR, Galli SJ: Mast cells as a source of multifunctional cytokines. *Immunol Today* 11:458–464, 1990
10. Ruoss SJ, Hartmann T, Caughey GH: Mast cell tryptase is a mitogen for cultured fibroblasts. *J Clin Invest* 88:493–499, 1991
11. Gruber BL, Kew RR, Jelaska A, *et al*: Human mast cells activate fibroblasts: Tryptase is a fibrogenic factor stimulating collagen messenger ribonucleic acid synthesis and fibroblast chemotaxis. *J Immunol* 158:2310–2317, 1997
12. Gordon JR, Galli SJ: Promotion of mouse fibroblast collagen gene expression by mast cells stimulated via the Fc epsilon RI. Role for mast cell-derived transforming growth factor beta and tumor necrosis factor alpha. *J Exp Med* 180:2027–2037, 1994
13. Thompson HL, Burbelo PD, Gabriel G, *et al*: Murine mast cells synthesize basement membrane components. A potential role in early fibrosis. *J Clin Invest* 87:619–623, 1991
14. Ehara T, Shigematsu H: Contribution of mast cells to the tubulointerstitial lesions in IgA nephritis. *Kidney Int* 54:1675–1683, 1998
15. Hiromura K, Kurosawa M, Yano S, *et al*: Tubulointerstitial mast cell infiltration in glomerulonephritis. *Am J Kidney Dis* 32:593–599, 1998
16. Roberts IS, Brenchley PE: Mast cells: The forgotten cells of renal fibrosis. *J Clin Pathol* 53:858–862, 2000
17. Toth T, Toth-Jakatics R, Jimi S, *et al*: Mast cells in rapidly progressive glomerulonephritis. *J Am Soc Nephrol* 10:1498–1505, 1999
18. Ruger BM, Hasan Q, Greenhill NS, *et al*: Mast cells and type VIII collagen in human diabetic nephropathy. *Diabetologia* 39:1215–1222, 1996
19. Lajoie G, Nadasdy T, Laszik Z, *et al*: Mast cells in acute cellular rejection of human renal allografts. *Mod Pathol* 9:1118–1125, 1996
20. Yamada M, Ueda M, Naruko T, *et al*: Mast cell chymase expression and mast cell phenotypes in human rejected kidneys. *Kidney Int* 59:1374–1381, 2001
21. Risdon RA, Sloper JC, de Wardener HE: Relationship between renal function and histological changes found in renal-biopsy specimens from patients with persistent glomerular nephritis. *Lancet* 2:363–366, 1968
22. Cameron JS: Tubular and interstitial factors in the progression of glomerulonephritis. *Pediatr Nephrol* 6:292–303, 1992
23. Niwa Y, Kasugai T, Ohno K, *et al*: Anemia and mast cell depletion in mutant rats that are homozygous at "white spotting (Ws)" locus. *Blood* 78:1936–1941, 1991
24. Tsujimura T, Hirota S, Nomura S, *et al*: Characterization of *Ws* mutant allele of rats: A 12-base deletion in tyrosine kinase domain of *c-kit* gene. *Blood* 78:1942–1946, 1991
25. Onoue H, Maeyama K, Nomura S, *et al*: Absence of immature mast cells in the skin of Ws/Ws rats with a small deletion at tyrosine kinase domain of the c-kit gene. *Am J Pathol* 142:1001–1007, 1993
26. Jones CL, Buch S, Post M, *et al*: Pathogenesis of interstitial fibrosis in chronic purine aminonucleoside nephrosis. *Kidney Int* 40:1020–1031, 1991
27. Chomczynski P, Sacchi N: Single-step method of RNA isolation by acid guanidinium thiocyanate-phenol-chloroform extraction. *Anal Biochem* 162:156–159, 1987
28. Ou ZL, Natori Y, Doi N, *et al*: Competitive reverse transcription-polymerase chain reaction for determination of rat CC and C chemokine mRNAs. *Anal Biochem* 261:227–229, 1998
29. Kivirikko KI, Laitinen O, Prockop DJ: Modifications of a specific assay for hydroxyproline in urine. *Anal Biochem* 19:249–255, 1967
30. Gibson S, Miller HR: Mast cell subsets in the rat distinguished immunohistochemically by their content of serine proteinases. *Immunology* 58:101–104, 1986
31. Gibson S, Mackeller A, Newlands GF, *et al*: Phenotypic expression of mast cell granule proteinases. Distribution of mast cell proteinases I and II in the rat digestive system. *Immunology* 62:621–627, 1987
32. Powell DW, Mifflin RC, Valentich JD, *et al*: Myofibroblasts. I. Paracrine cells important in health and disease. *Am J Physiol* 277:C1–9, 1999
33. Weigert C, Brodbeck K, Haring HU, *et al*: Low-molecular-weight heparin prevents high glucose- and phorbol ester-induced TGF-beta 1 gene activation. *Kidney Int* 60:935–943, 2001
34. Tei H, Kasugai T, Tsujimura T, *et al*: Characterization of cultured mast cells derived from *Ws/Ws* mast cell-deficient rats with a small deletion at tyrosine kinase domain of *c-kit*. *Blood* 83:916–925, 1994
35. Remuzzi G, Bertani T: Pathophysiology of progressive nephropathies. *N Engl J Med* 339:1448–1456, 1998
36. Okazaki T, Hirota S, Xu ZD, *et al*: Increase of mast cells in the liver and lung may be associated with but not a cause of fibrosis: Demonstration using mast cell-deficient Ws/Ws rats. *Lab Invest* 78:1431–1438, 1998
37. Mori H, Kawad K, Zhang P, *et al*: Bleomycin-induced pulmonary fibrosis in genetically mast cell-deficient WBB6F1-W/Wv mice and mechanism of the suppressive effect of tranilast, an antiallergic drug inhibiting mediator release from mast cells, on fibrosis. *Int Arch Allergy Appl Immunol* 95:195–201, 1991
38. Sugihara A, Tsujimura T, Fujita Y, *et al*: Evaluation of role of mast cells in the development of liver fibrosis using mast cell-deficient rats and mice. *J Hepatol* 30:859–867, 1999
39. Everett ET, Pablos JL, Harley RA, *et al*: The role of mast cells in the development of skin fibrosis in tight-skin mutant mice. *Comp Biochem Physiol A Physiol* 110:159–165, 1995
40. Yamamoto T, Takahashi Y, Takagawa S, *et al*: Animal model of sclerotic skin. II. Bleomycin induced scleroderma in genetically mast cell deficient WBB6F1-W/Wv mice. *J Rheumatol* 26:2628–2634, 1999
41. Lukacs NW, Hogaboam C, Chensue SW, *et al*: Type 1/type 2 cytokine paradigm and the progression of pulmonary fibrosis. *Chest* 120:5S–8S, 2001
42. Metcalfe DD, Baram D, Mekori YA: Mast cells. *Physiol Rev* 77:1033–1079, 1997

43. Del VECCHIO PJ, BIZIOS R, HOLLERAN LA, *et al*: Inhibition of human scleral fibroblast proliferation with heparin. *Invest Ophthalmol Vis Sci* 29:1272–1276, 1988
44. KONDO S, KAGAMI S, KIDO H, *et al*: Role of mast cell tryptase in renal interstitial fibrosis. *J Am Soc Nephrol* 12:1668–1676, 2001
45. YARD BA, CHORIANOPOULOS E, HERR D, *et al*: Regulation of endothelin-1 and transforming growth factor-beta1 production in cultured proximal tubular cells by albumin and heparan sulphate glycosaminoglycans. *Nephrol Dial Transplant* 16:1769–1775, 2001
46. MULLER GA, MARKOVIC-LIPKOVSKI J, FRANK J, *et al*: The role of interstitial cells in the progression of renal diseases. *J Am Soc Nephrol* 2:S198–S205, 1992

J Hum Genet (2004) 49:629–634
DOI 10.1007/s10038-004-0199-3

ORIGINAL ARTICLE

Hajime Nawata · Senji Shirasawa · Naoki Nakashima
Eiichi Araki · Jun Hashiguchi · Seibei Miyake
Teruaki Yamauchi · Kazuyuki Hamaguchi
Hironobu Yoshimatsu · Haruo Takeda
Hideo Fukushima · Takayuki Sasahara
Kohei Yamaguchi · Noriyuki Sonoda · Tomoko Sonoda
Masahiro Matsumoto · Yoshiya Tanaka
Hidekatsu Sugimoto · Hirotaka Tsubouchi
Toyoshi Inoguchi · Toshihiko Yanase
Nakayasu Wake · Kenziro Narazaki · Takashi Eto
Fumio Umeda · Mitsuhiro Nakazaki · Junko Ono
Takashi Asano · Yasuko Ito · Shoichi Akazawa
Iwaho Hazegawa · Nobuyuki Takasu
Moritsugu Shinohara · Takeshi Nishikawa
Seiho Nagafuchi · Toshimitsu Okeda
Katsumi Eguchi · Masanori Iwase · Mayuko Ishikawa
Masayuki Aoki · Naoto Keicho · Norihiro Kato
Kazuki Yasuda · Ken Yamamoto · Takehiko Sasazuki

Genome-wide linkage analysis of type 2 diabetes mellitus reconfirms the susceptibility locus on 11p13–p12 in Japanese

Received: 9 July 2004 / Accepted: 9 August 2004 / Published online: 14 October 2004

Abstract Type 2 diabetes mellitus is a heterogeneous disorder, and the development of type 2 diabetes mellitus is associated with both insulin secretion defect and insulin resistance. The primary metabolic defect leading to type 2 diabetes mellitus has been thought to be varied among populations, especially in Japanese and Caucasians. Here, we have done the genome-wide scan for type 2 diabetes mellitus using 102 affected Japanese sib-pairs to identify the genetic factors predisposing to type 2 diabetes mellitus. Nonparametric linkage analysis showed one suggestive evidence for linkage to 11p13–p12 [*D11S905*: two-point maximum LOD score (MLS) of 2.89 and multipoint MLS of 2.32] and one nominally significant evidence for linkage to 6q15–q16 (*D6S462*: two-point MLS of 2.02). Interestingly, the 11p13–p12 region was reported to be a susceptibility locus for Japanese type 2 diabetes mellitus with suggestive evidence of linkage, and *D11S905* was within 5 cM to *D11S935* with the highest MLS in the previous linkage analysis reported. The only overlapped susceptibility region with suggestive evidence of linkage for Japanese type 2 diabetes mellitus was *D11S935–D11S905* among

H. Nawata · N. Sonoda · H. Tsubouchi · T. Inoguchi
T. Yanase · T. Eto
Department of Medicine and Bioregulatory Science,
Graduate School of Medical Sciences, Kyushu University,
Fukuoka, Japan

S. Shirasawa · M. Ishikawa
Department of Pathology, Research Institute,
International Medical Center, Tokyo, Japan

N. Nakashima
Department of Medical Informatics,
Kyushu University Hospital, Fukuoka, Japan

E. Araki · T. Nishikawa
Department of Metabolic Medicine,
Faculty of Medical and Pharmaceutical Sciences,
Kumamoto University, Kumamoto, Japan

J. Hashiguchi
Tenposan Clinic, Kagoshima, Japan

S. Miyake
Sasebo Central Hospital, Nagasaki, Japan

T. Yamauchi
Yukuhashi Central Hospital, Fukuoka, Japan

K. Hamaguchi · H. Yoshimatsu
Department of Internal Medicine 1,
Faculty of Medicine, Oita University, Oita, Japan

H. Takeda
Yatsushiro General Hospital, Kumamoto, Japan

H. Fukushima
Public Tamana Central Hospital, Kumamoto, Japan

T. Sasahara
Omuta Tenryo Hospital, Fukuoka, Japan

K. Yamaguchi
Oita Prefectural Hospital, Oita, Japan

T. Sonoda
Sonoda Clinic, Kagoshima, Japan

M. Matsumoto
Kitakyushu Municipal Medical Center, Fukuoka, Japan

Y. Tanaka
First Department of Internal Medicine, School of Medicine,
University of Occupational & Environmental Health,
Fukuoka, Japan

H. Sugimoto
Sugimoto Clinic, Fukuoka, Japan

N. Wake
National Health Insurance Takachiho Town Hospital,
Miyazaki, Japan

K. Narazaki
Narazaki Clinic, Fukuoka, Japan

F. Umeda
Diabetology and Endocrinology Division of Internal Medicine,
Fukuoka Medical Association Hospital, Fukuoka, Japan

M. Nakazaki
Department of Cardiovascular,
Respiratory & Metabolic Medicine
Graduate School of Medicine, Kagoshima University,
Kagoshima, Japan

J. Ono
Department of Laboratory Medicine,
School of Medicine,
Fukuoka University, Fukuoka, Japan

T. Asano
First Department of Internal Medicine,
School of Medicine,
Fukuoka University, Fukuoka, Japan

Y. Ito
Furugou Clinic, Oita, Japan

S. Akazawa
Shin-Koga Hospital, Fukuoka, Japan

I. Hazegawa
Kamiamakusa General Hospital, Kumamoto, Japan

N. Takasu
Department of Endocrinology and Metabolism,
Faculty of Medicine, University of the Ryukyus,
Okinawa, Japan

M. Shinohara
National Health Insurance Matsubase Town Hospital,
Kumamoto, Japan

S. Nagafuchi
Department of Medicine and Biosystemic Science,
Graduate School of Medical Sciences,
Kyushu University, Fukuoka, Japan

T. Okeda
Shin-Kokura Hospital, Fukuoka, Japan

K. Eguchi
First Department of Internal Medicine,
Graduate School of Biomedical Sciences,
Nagasaki University, Nagasaki, Japan

M. Iwase
Department of Medicine and Clinical Science,
Graduate School of Medical Sciences,
Kyushu University, Fukuoka, Japan

M. Aoki · K. Yamamoto
Medical Institute of Bioregulation, Kyushu University,
Fukuoka, Japan

N. Keicho · N. Kato · K. Yasuda
Research Institute,
International Medical Center of Japan,
Tokyo, Japan

T. Sasazuki (✉)
International Medical Center of Japan, 1-21-1 Toyama,
Shinjuku-ku, Tokyo 162-8655, Japan
E-mail: sasazuki@nciryo.hosp.go.jp
Tel.: +81-3-32027181
Fax: +81-3-52730113

the three reports including this study. These results taken together suggest that a susceptibility gene for type 2 diabetes mellitus in Japanese will reside in 11p13–p12.

Keywords Type 2 diabetes mellitus · Japanese · Affected sib-pairs · Linkage · Chromosome 11p

Introduction

Type 2 diabetes mellitus is one of the most common diseases, and its prevalence is dramatically increasing worldwide (Zimmet et al. 2001). Type 2 diabetes mellitus is a heterogeneous disorder, and the development of type 2 diabetes mellitus is associated with both insulin secretion defect and insulin resistance. Japanese patients with type 2 diabetes mellitus were reported to be characterized by a lower body mass index (BMI) and lower fasting insulin levels than other populations (Ehm et al. 2000). Insulin secretion defect is thought to be the primary defect in Japanese (Kadowaki et al. 1984) whereas impaired insulin sensitivity is the first metabolic defect predisposing to the development of type 2 diabetes mellitus in Caucasians (Martin et al. 1992). These findings suggest that Japanese individuals with type 2 diabetes mellitus will have a different genetic risk factor, which affects the responsiveness of insulin secretion to glucose, from other populations. Therefore, we need to identify the susceptibility genes for the development of type 2 diabetes mellitus in Japanese to start a primary prevention based on genetic information and to develop the personalized medicine for type 2 diabetes mellitus in Japanese. So far, two whole-genome linkage analyses were carried out using 224 affected sib-pairs (ASPs) from 159 Japanese families (Mori et al. 2002) and 256 ASPs from 164 Japanese families (Iwasaki et al. 2003), besides the analysis of 45 ASPs from 18 Japanese American families (Ehm et al. 2000). The Japanese people may have advantages in the genetic analysis of polygenic disorders like diabetes since they are supposed to be a relatively homogeneous population. However, the two previous reports on the ASP analysis in Japanese did not give good overlapping regions, except for 6p and 2q, and it has been argued that the replication by the third panel is indispensable for genetic susceptibility loci in Japanese. Here, we have carried out the third whole-genome linkage analysis on 102 ASPs from 102 Japanese families to identify the susceptibility loci for the development of type 2 diabetes mellitus.

Subjects and methods

One hundred and two ASPs with type 2 diabetes mellitus from 102 families were collected mainly from the Kyushu region in southwestern Japan. Parents and other siblings were not available in this study. The participants were interviewed and examined and gave written informed consent. This project was approved by the ethics committees of the related institutes. The diagnosis of type 2 diabetes mellitus was made based on the American Diabetes Association's 1997 criteria (Expert

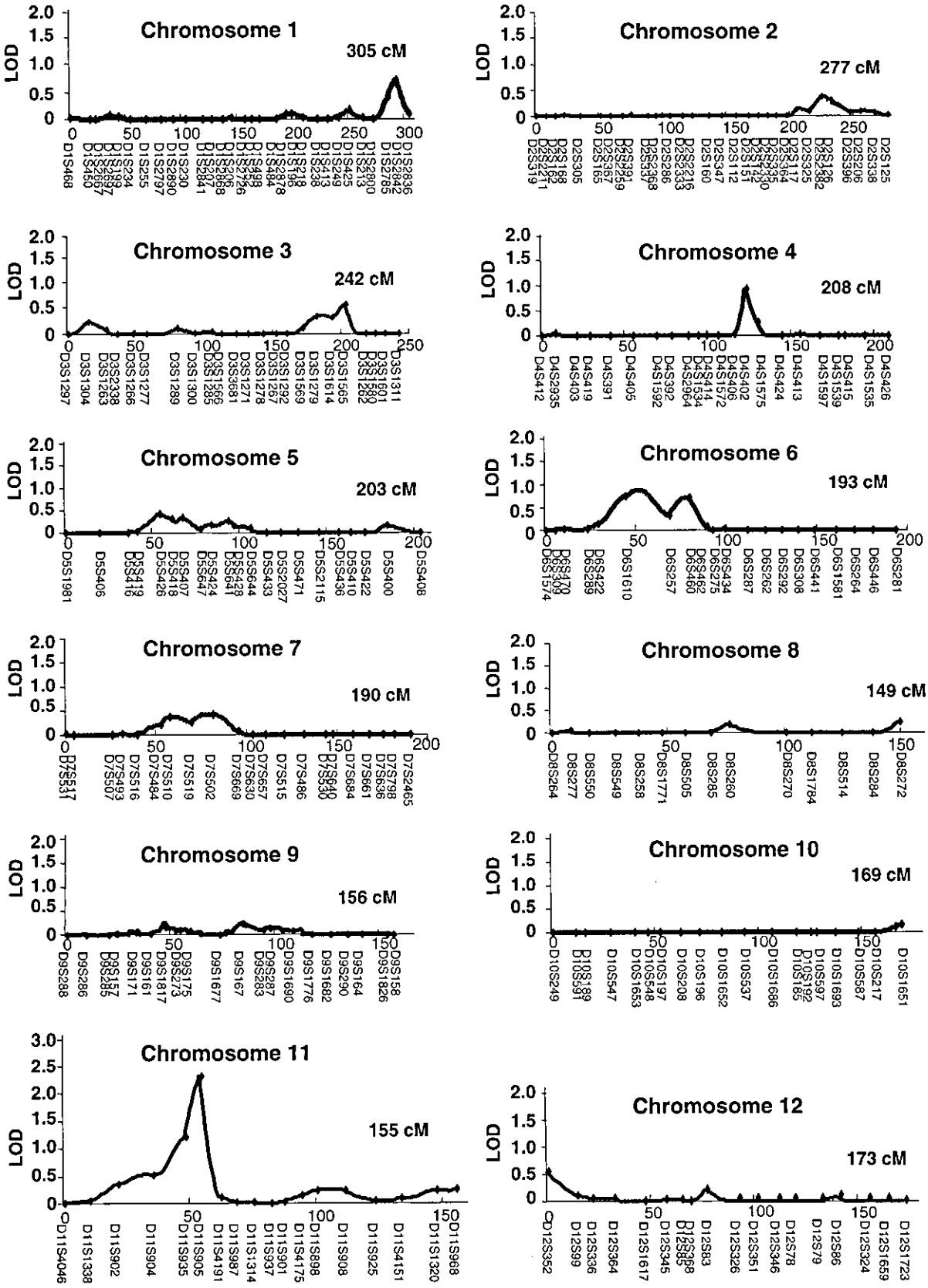

Fig. 1 Multipoint LOD score map of type 2 diabetes mellitus by linkage analysis of 382 markers in 102 affected sib-pairs. The *horizontal axis* is cM position from the p-terminal end of the chromosome

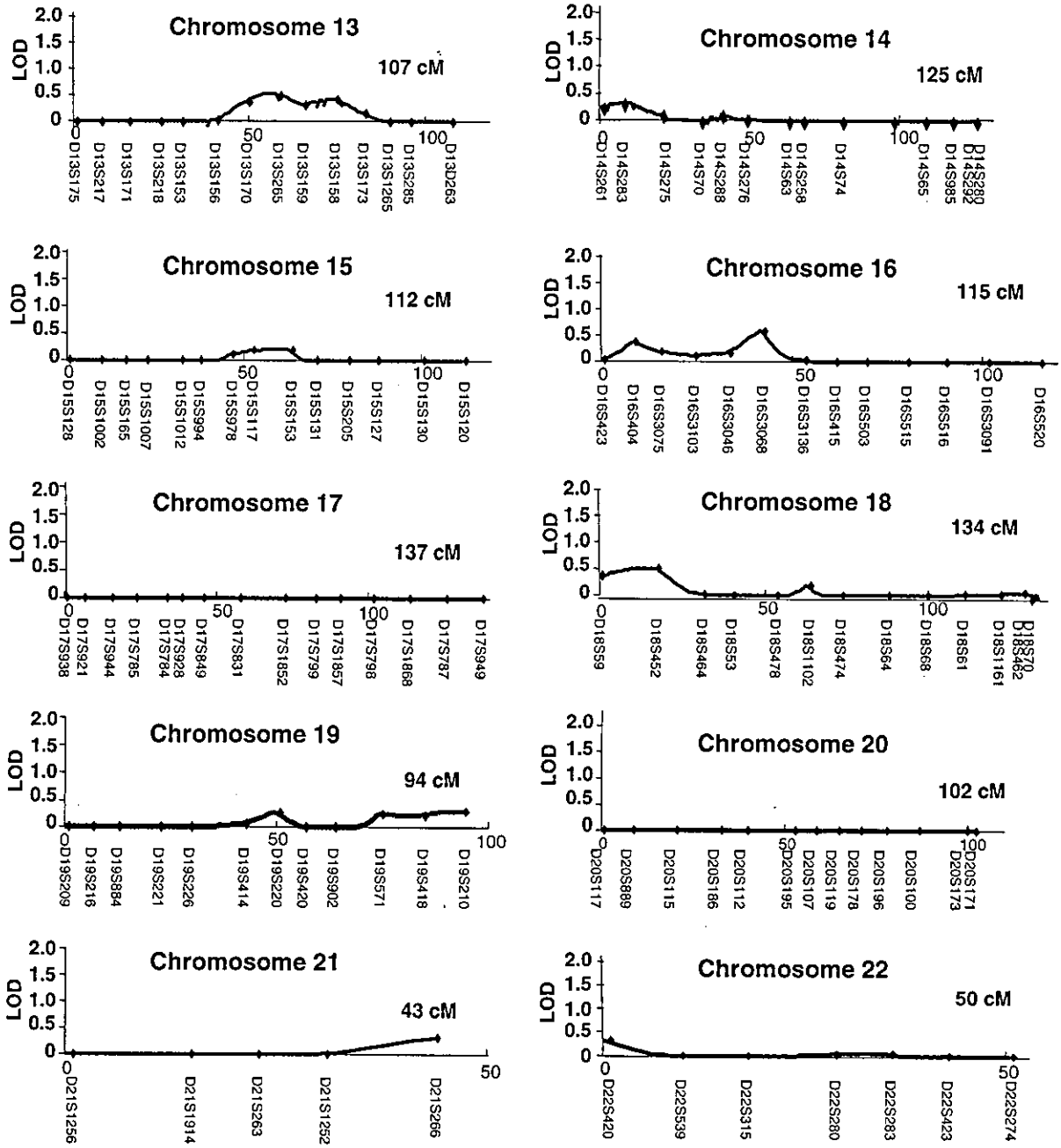

Fig. 1 (Continued)

Committee on the Diagnosis and Classification of Diabetes Mellitus 1997).

Genomic DNA was isolated from peripheral blood cells using QIAamp DNA Blood Midi Kits (Qiagen). Autosomal whole-genome screening of 382 microsatellite markers (ABI PRISM Linkage Mapping Set Version 2.5-MD10) was performed using an ABI 3730 automatic sequencer (Applied Biosytems). Analyses and assignment of the marker alleles were done with ABI PRISM GeneMapper Software Version 3.0, and 376 markers were available for the linkage analysis. Nonparametric two-point and multipoint linkage analyses were performed with the MAPMAKER/SIBS program (Kruglyak and Lander 1995), as described (Sakai et al. 2001). Heterozygosities of the markers were estimated

Table 1 Results of linkage analysis of type 2 diabetes mellitus and markers showing evidence of linkage

Marker	cM[a]	Analysis	MLS	*P*
D6S462	89	Two-point	2.02	0.0097
D11S905	54	Two-point	2.89	0.0013
		Multipoint	2.32	0.0048

[a]The distance of the marker form the p-terminal end of the chromosome in cM

with Merlin program (Abecasis et al. 2002) for all individuals.

Results and discussion

Whole autosomal genome linkage analysis using the ASP method with 382 microsatellite markers was carried out on 102 Japanese ASPs with type 2 diabetes mellitus. In this study, the average heterozygosity of the markers used was 0.72. Multipoint linkage analysis at all autosomal chromosomes using the MAPMAKER/SIBS program revealed only one region on chromosome 11p where the MLS was > 1 (Fig. 1). The highest multipoint MLS was 2.32 ($P = 0.0048$) at *D11S905* (Fig. 1, Table 1). On the other hand, two-point linkage analysis revealed two markers, *D11S905* (MLS = 2.89, $P = 0.0013$) and *D6S462* (MLS = 2.02, $P = 0.0097$), with evidence of linkage to type 2 diabetes mellitus (Table 1). Although the heterozygosity of *D11S905* was 0.30 in this study, it was 0.75 and 0.60 in our two reports using ASPs (Sakai et al. 2001; Aoki et al. 2004), indicating that *D11S905* itself will be useful in the genetic analysis in terms of heterozygosity in the Japanese population, and particular alleles of *D11S905* might be associated with type 2 diabetes mellitus. The 11p13–p12 region was reported to be linked to Japanese type 2 diabetes mellitus specifically, in which multipoint analysis showed the highest MLS of 3.08 near *D11S935* (Mori et al. 2002). The distance between *D11S905* and *D11S935* is about 5 cM. These findings together suggest that the 11p13–p12 region will be a susceptibility region for Japanese type 2 diabetes mellitus.

In addition to *D11S905*, one nominally significant evidence of linkage was detected at *D6S462* (MLS of 2.02) by two-point analysis. However, the multipoint MLS at *D6S462* was 0.08, and two other reports did not show evidence of linkage to this region (Mori et al. 2002; Iwasaki et al. 2003), suggesting that 6q15–q16 might not be a susceptibility region for type 2 diabetes mellitus. Two susceptibility regions for type 2 diabetes mellitus in Japanese, chromosome 2 (236.8 cM) and chromosome 6 (42.2 cM), were reported to be overlapped between the two previous linkage studies (Iwasaki et al. 2003). However, the MLS at these two loci were < 1 (Iwasaki et al. 2003). Among the three reports including this study, the overlapped susceptibility region with suggestive evidence of linkage for Japanese type 2 diabetes mellitus was *D11S935–D11S905* only.

In conclusion, we have reconfirmed that the evidence of linkage for type 2 diabetes mellitus in Japanese to 11p13–p12 and 11p13–p12 will be a promising region for future studies on identification of susceptibility genes for type 2 diabetes mellitus in Japanese.

Acknowledgements We thank all patients for participating in this study, T. Amano in Kyushu University and T. Baba in SRL, Inc., for collecting the samples, and A. Murakami, E. Yachi, K. Ohki, and T. Fujimoto for technical assistance. This work was supported by the Program for Promotion of Fundamental Studies in Health Sciences of Pharmaceuticals and Medical Devices Agency (PMDA).

Appendix

Collaborating groups listed in alphabetic order: Nobuyuki Abe (Abe Diabetes Clinic), Katsumi Eguchi (Nagasaki University), Nobuaki Fujio (Beppu Medical Center), Masafumi Haji (Kyushu Rosai Hospital), Mine Harada (Kyushu University), Sinsuke Hiramatsu (Kyushu Medical Center), Mitsuo Iida (Kyushu University), Minako Imamura (Kyushu University), Hidehiro Ishii (Kitakyushu Municipal Medical Center), Eiji Kawasaki (Nagasaki University), Kunihisa Kobayashi (Kyushu University), Ichiro Komiya (University of the Ryukyus), Shiori Kondo (Matsuyama Red Cross Hospital), Yasuko Kono (Imamura Hospital), Nobuyuki Koriyama (Kagoshima University), Minoru Kuriyama (Social Health Insurance Inatsuki Hospital), Kazunari Matsumoto (Sasebo Central Hospital), Kazuo Mimura (Fukuoka Medical Association Hospital), Isao Morimoto (Inoue Hospital), Mieko Nakayama (Kyushu University), Shyoichi Natori (Aso Iizuka Hospital), Yosuke Okada (University of Occupational & Environmental Health), Haruka Sasaki (Fukuoka University), Naotaka Sekiguchi (Kyushu University), Yasunori Sera (Sasebo Central Hospital), Michio Shimabukuro (University of the Ryukyus), Yuji Tajiri (Fukuoka Medical Association Hospital), Chuwa Tei (Kagoshima University), Maiko Tsuda (Kitakyushu Municipal Medical Center), Takero Uemura (Yatsushiro General Hospital), Eiji Kawasaki (Nagasaki University).

References

Abecasis GR, Cherny SS, Cookson WO, Cardon LR (2002) Merlin-rapid analysis of dense genetic maps using sparse gene flow trees. Nat Genet 30:97–101

Aoki M, Yamamura Y, Noshiro H, Sakai K, Yokota J, Kohno T, Tokino T, Ishida S, Ohyama S, Ninomiya I, Uesaka K, Kitajima M, Shimada S, Matsuno S, Yano M, Hiratsuka M, Sugimura H, Itoh F, Minamoto T, Machara Y, Takenoshita S, Aikou T, Katai H, Yoshimura K, Takahashi T, Akagi K, Sairenji M, Yamamoto K, Sasazuki T (2004) A full genome scan for gastric cancer. J Med Genet (in press)

Ehm MG, Karnoub MC, Sakul H, Gottschalk K, Holt DC, Weber JL, Vaske D, Briley L, Kopf J, McMillen P, Nguyen Q, Reisman M, Lai EH, Joslyn G, Shepherd NS, Bell C, Wagner MJ, Burns DK, ADA GENNID Study Group (2000) Genomewide search for type 2 diabetes mellitus susceptibility genes in four American populations. Am J Hum Genet 66:1871–1881

Expert Committee on the Diagnosis and Classification of Diabetes Mellitus (1997) Report of the expert committee on the diagnosis and classification of diabetes mellitus. Diabetes Care 20:1183–1197

Iwasaki N, Cox NJ, Wang Y-Q, Schwaz PEH, Bell GI, Honda M, Imura M, Ogata M, Saito M, Kamatani N, Iwamoto Y (2003) Mapping genes influencing type 2 diabetes mellitus risk and BMI in Japanese subjects. Diabetes 52:209–213

Kadowaki T, Miyake Y, Hagura R, Akanuma Y, Kajinuma H, Kuzuya N, Takaku F, Kosaka K (1984) Risk factors for worsening to diabetes in subjects with impaired glucose tolerance. Diabetologia 26:44–49

Kruglyak L, Lander ES (1995) Complete multipoint sib-pair analysis of qualitative and quantitative traits. Am J Hum Genet 57:439–454

Martin BC, Warram JH, Krolewski AS, Bergman RN, Soeldner JS, Kahan CR (1992) Lancet 340:925–929

Mori Y, Otabe S, Dina C, Yasuda K, Populaire C, Lecoeur C, Vatin V, Durand E, Hara K, Okada T, Tobe K, Boutin P, Kadowaki T, Froguel P (2002) Genome-wide search for type 2 diabetes mellitus in Japanese affected sib-pairs confirms susceptibility genes on 3q, 15q, and 20q and identifies two new candidate loci on 7p and 11p. Diabetes 51:1247–1255

Sakai K, Shirasawa S, Ishikawa N, Ito K, Tamai H, Kuma K, Akamizu T, Tanimura M, Furugaki K, Yamamoto K, Sasazuki T (2001) Identification of susceptibility loci for autoimmune thyroid disease to 5q31–q33 and Hashimoto's thyroiditis to 8q23–q24 by multipoint affected sib-pair linkage analysis in Japanese. Hum Mol Genet 10:1379–1386

Zimmet P, Alberti KGMM, Shaw J (2001) Global and societal implications of the diabetes epidemic. Nature 414:782–787

Microbiol. Immunol., 49(2), 181–189, 2005

Editor-Communicated Paper

Susceptibility Loci to Coronary Arteritis in Animal Model of Kawasaki Disease Induced with *Candida albicans*-Derived Substances

Toshiaki Oharaseki*[,1], Yosuke Kameoka[2], Fumiaki Kura[3], Amanda S. Persad[4], Kazuo Suzuki[4], and Shiro Naoe[1]

[1]*Department of Pathology, Ohashi Hospital, Toho University School of Medicine, Meguro-ku, Tokyo 153–8515, Japan,* [2]*Division of Genetic Resources,* [3]*Department of Bacteriology, and* [4]*Department of Bioactive Molecules, National Institute of Infectious Diseases, Shinjuku-ku, Tokyo 162–8640, Japan*

Communicated by Dr. Hidechika Okada: Received November 26, 2004. Accepted December 13, 2004

Abstract: **We have established an animal model of coronary arteritis which is histopathologically similar to that observed in cases of Kawasaki disease (KD), is a well-known childhood vasculitis syndrome. Coronary arteritis in this mouse model has been induced by intraperitoneal injection of *Candida albicans*-derived substances (CADS). Arteritis varied by mouse strain with the highest incidence by 71.1% (27/38) found in C3H/HeN mice, but absent in CBA/JN mice (0%, 0/27), suggesting association of genomic background to develop the disease. The present study aims to elucidate the susceptibility loci associated with coronary arteritis by using this animal model. The association of the onset of arteritis with polymorphic microsatellite markers between the two strains was examined using one hundred and fifteen of N1 backcross progeny [(CBA×C3H)F1×C3H]. Based on our analysis, arteritis-susceptibility loci with suggestive linkage were mapped on *D1Mit171* and *D1Mit245* (map position 20.2 cM) on chromosome 1 (P=0.0019). These loci include several kinds of inflammatory cytokine receptors, such as interleukin 1 receptor and tumor necrosis factor receptor. We also found the cytokine response against CADS, levels of inflammatory cytokines interleukin-1β, tumor necrosis factor-α, and interleukin-6 in sera increased within 24 hr after CADS injection. Our results may indicate based on genomics that ligand-receptor interaction between these inflammatory cytokines and the receptors of these cytokines may affect the onset of arteritis.**

Key words: **Kawasaki disease, Arteritis, *Candida albicans*, Interleukin 1 receptor, Chromosome mapping**

Kawasaki disease (KD) is an acute febrile mucocutaneous syndrome with systemic vasculitis mainly affecting infants and small children. The principal symptoms of KD are fever, congestion of ocular conjunctivae, reddening of lips and oral mucosa, swelling and reddening of palms and soles followed by peeling of skin, swelling of cervical lymph nodes coincidentally with systemic vasculitis (9). Inflammation of medium-sized muscular arteries, especially the coronary artery, is commonly associated with this disease. Ischemic heart disease with thrombotic occlusion, originating from coronary arteritis is a severe complication of KD. Histopathologically, it was reported that arteritis defined as 'productive granulomatous inflammation' was typical in KD cases (15, 19). This type of inflammation consists of dense infiltration of both neutrophils and histiocytes accompanied with a few lymphocytes. Mechanisms of developing arteritis in the patients with KD

**Address correspondence to* Dr. Toshiaki Oharaseki, Department of Pathology, Ohashi Hospital, Toho University School of Medicine, 2–17–6 Ohashi, Meguro-ku, Tokyo 153–8515, Japan. Fax: +81–3–3468–1283. E-mail: oharasek@muc.biglobe.ne.jp

Abbreviations: CADS, *Candida albicans* derived substances; cM, centi-morgan; ELISA, enzyme-linked immunosorbent assay; EvG, Elastica van Gieson; HE, hematoxylin and eosin; IFN-γ, interferon-γ; IL, interleukin; *Il1r1*, interleukin-1 receptor type 1; *Il1r2*, interleukin-1 receptor type 2; KD, Kawasaki disease; MCLS-6, mucocutaneous lymphnode syndrome-6; MPO, myeloperoxidase; MPO-ANCA, myeloperoxidase-antineutrophilic cytoplasmic antibody; PCR, polymerase chain reaction; QTL, quantitative trait of loci; TNF-α, tumor necrosis factor α; *Tnfrsf1b*, TNF receptor superfamily member 1b; *Tnfrsf8*, TNF receptor superfamily member 8; *Tnfrsf9*, TNF receptor superfamily member 9.

remain to be determined; however, there are some reports that coronary arteritis is affected by genetic polymorphism of several kinds of inflammatory cytokines, such as tumor necrosis factor α (TNF-α) (8), and interleukin-6 (IL-6) (7). Appropriate animal models of KD will allow for the clarification of the mechanisms governing the development of arteritis, and possibly, specific treatments for this disease. One of the animal models of arteritis that exist is the MRL/lpr mouse model. It is the standard animal model for studying systemic lupus erythematosus, with a common affliction to spontaneous arteritis. In MRL/lpr mice, some genes associated with arteritis have been elucidated (5). Recently, it was reported that arteritis in different tissues were under the control of different susceptibility loci (21).

Some infectious microorganisms, such as *Staphylococcus aureus* (11), *Streptococcus sanguis* (16), *Streptococcus pyogenes* (22), and *Rickettsia* (6) have been considered likely etiology candidates for this disease, though the primary causes remain unclear. These microorganisms are considered to act as the initial trigger for the development of arteritis in the patients with KD. Therefore, the initial trigger by an infectious microorganism is necessary for ideal model of KD to induce arteritis. However, this spontaneous arteritis model may not be well suited as an animal model for KD. On the other hand, Murata (13) has established a unique arteritis model that has been evaluated as an animal model of KD. In this model, arteritis induction is ascertained by injecting mice with alkaline extract of *Candida albicans* as an experimental arteritis. It should be noted that the quantity of this yeast was observed to be in elevated in stool samples of KD patients (14). The histology of this experimental arteritis model is similar to that of an autopsy case of KD (2). In this model, genetics in mice may have an influence on the development of arteritis. It was shown that the incidence of coronary arteritis varied by mouse strain, with the C3H/HeN mice having the highest incidence and coronary arteritis being absent in CBA/JN strains (20).

To identify susceptibility loci to the coronary arteritis, we analyzed coronary arteritis in [(CBA/JN×C3H/HeN) ×C3H/HeN]N1 backcross progeny. The evidence presented herein shows that the susceptibility loci are linked to genes of several inflammatory cytokine receptors found in the coronary artery.

Materials and Methods

Chemicals. Sabouraud-2% dextrose broth (MERCK, Darmstadt, Germany) was used as culture medium. Sodium chloride, potassium hydroxide, acetic acid, ethanol, acetone, diethyl ether (Wako Pure Chemical Industries, Ltd., Osaka, Japan) and *n*-octyl alcohol (Kanto Chemical Co., Tokyo) were used for polysaccharide extraction from the cell wall of *C. albicans*.

Genomic DNA was isolated from whole blood obtained from the tail of animals using the QIAamp DNA mini kit (Qiagen, Hilden, Germany). FAM labeled primers for microsatellite markers were purchased from SIGMA Genosys Japan (Ishikari, Japan). Amplification and labeling of each microsatellite locus were performed by using Z-*Taq* polymerase (TaKaRa, Kyoto, Japan).

Animals. Mice, CBA/JNCrj (CBA/JN) and C3H/HeNCrj (C3H/HeN), were purchased from Charles River Japan (Astugi, Japan). Using C3H/HeN and CBA/JN strains, (C3H/HeN female×CBA/JN male)F1, (CBA/JN female×C3H/HeN male)F1, and [(CBA/JN×C3H/HeN)F1×C3H/HeN]N1 were prepared. N1 backcross progeny, 4-week-old males, were used for the linkage analysis (n=115). These mice were housed in a specific pathogen-free animal quarter and cared for under strict ethical guidelines.

Preparation of alkaline extract of C. albicans *(CADS).* CADS were prepared as follows. *C. albicans* (strain MCLS-6) isolated from the feces of patients with typical Kawasaki disease, was cultured in Sabouraud's dextrose medium with 2% glucose at 37 C. After a 72-hr incubation period, the yeast was harvested by centrifugation and extracted sequentially with boiling water, 0.1 M, and 0.5 M potassium hydroxide. After neutralization with acetic acid and dialysis against distilled water for 3 days, the extract was precipitated with ethanol. Four milligrams of the CADS, suspended in 0.2 ml of phosphate-buffered saline without calcium and magnesium (PBS(−)), were prepared as the inoculants.

Experimental schedule. Inoculation was conducted as described in the previous procedures (13). Namely, mice were injected once daily with 0.2 ml of inoculate intraperitoneally for 5 consecutive days during the first and fifth week. Each mouse was sacrificed with carbon dioxide asphyxiation at the ninth week and autopsied.

Histopathological evaluation of arteritis. The following visceral organs were obtained for histopathological examination: heart, aorta, kidney, lung, liver, pancreas, spleen, thymus, testis, muscle of hind leg, and spine. These specimens were fixed in 10% formalin and embedded in paraffin. Hematoxylin and eosin (HE) and Elastica van Gieson (EvG) stains were performed by routine histological techniques. Arteritis in individual mice was determined using light microscopy. A mouse with inflammation involving all layers of coronary artery and/or the aortic root was considered positive for coronary arteritis and used for linkage analysis.

Microsatellite markers. Two hundred and fifty-six markers (Fig. 1) were used for the linkage analysis between C3H/HeN and CBA/JN mice. Amplification and labeling of specific microsatellite loci were performed by using the polymerase chain reaction (PCR) with FAM labeled primers. Amplified DNA was analyzed with automated fragment analyzer ABI3700 and genotyped by Genescan software (Applied Biosystems, Japan).

Linkage analysis. Genotype distribution was compared among affected and non-affected N1 mice. Since the trait distribution was similar, we performed non-

Chromosome 1 (53)									
	D1Mcg101	D1Mcg2	D1Mcg3	D1Mcg4	D1Mcg6	D1Mit120	D1Mit121	D1Mit160	D1Mit160
	D1Mit161	D1Mit167	D1Mit17	D1Mit171	D1Mit180	D1Mit19	D1Mit200	D1Mit211	D1Mit230
	D1Mit24	D1Mit242	D1Mit245	D1Mit251	D1Mit296	D1Mit3	D1Mit303	D1Mit316	D1Mit318
	D1Mit321	D1Mit322	D1Mit363	D1Mit372	D1Mit373	D1Mit374	D1Mit380	D1Mit410	D1Mit427
	D1Mit429	D1Mit430	D1Mit431	D1Mit432	D1Mit465	D1Mit518	D1Mit52	D1Mit52.2	D1Mit520
	D1Mit58	D1Mit64	D1Mit66	D1Mit67	D1Mit7	D1Mit70	D1Mit73	D1Mit75	
Chromosome 2 (25)									
	D2Mit106	D2Mit110	D2Mit139	D2Mit166	D2Mit169	D2Mit194	D2Mit200	D2Mit206	D2Mit226
	D2Mit255	D2Mit258	D2Mit265	D2Mit304	D2Mit305	D2Mit307	D2Mit311	D2Mit413	D2Mit443
	D2Mit456	D2Mit457	D2Mit496	D2Mit51	D2Mit6	D2Mit91	D2Mit92		
Chromosome 3 (11)									
	D3Mit200	D3Mit203	D3Mit230	D3Mit28	D3Mit29	D3Mit3	D3Mit305	D3Mit323	D3Mit361
	D3Mit46	D3Mit90							
Chromosome 4 (37)									
	D4Mit116	D4Mit122	D4Mit126	D4Mit134	D4Mit146	D4Mit169	D4Mit18	D4Mit180	D4Mit181
	D4Mit190	D4Mit203	D4Mit219	D4Mit225	D4Mit226	D4Mit227	D4Mit234.2	D4Mit251	D4Mit255
	D4Mit26	D4Mit27	D4Mit272	D4Mit285	D4Mit310	D4Mit33	D4Mit331	D4Mit336	D4Mit348
	D4Mit354	D4Mit357	D4Mit42	D4Mit43	D4Mit45	D4Mit65	D4Mit71	D4Mit81	D4Mit84
	D4Nds3								
Chromosome 5 (22)									
	D5Mit10	D5Mit101	D5Mit108	D5Mit115	D5Mit13	D5Mit134	D5Mit23	D5Mit233	D5Mit239
	D5Mit254	D5Mit26	D5Mit291	D5Mit297	D5Mit314	D5Mit338	D5Mit348	D5Mit371	D5Mit406
	D5Mit425	D5Mit65	D5Mit79	D5Mit93					
Chromosome 6 (4)									
	D6Mit345	D6Mit366	D6Mit8	D6Mit254					
Chromosome 7 (5)									
	D7Mit232	D7Mit259	D7Mit27	D7Mit39	D7Nds5				
Chromosome 8 (3)									
	D8Mit14	D8Mit224	Mt2(D8Mit15)						
Chromosome 9 (3)									
	Cyp1a2(ch#9)		D9Mit2	D9Mit279					
Chromosome 10 (16)									
	D10Mit115	D10Mit134	D10Mit15	D10Mit150	D10Mit186	D10Mit20	D10Mit209	D10Mit214	D10Mit230
	D10Mit261	D10Mit266	D10Mit282	D10Mit297	D10Mit313	D10Mit36	D10Mit61		
Chromosome 11 (3)									
	D11Mit157	D11Mit2	Hoxb(Ch#11)						
Chromosome 12 (4)									
	D12Mit158	D12Mit190	D12Mit231	D12Mit292					
Chromosome 13 (9)									
	D13Mit110	D13Mit186	D13Mit24	D13Mit253	D13Mit26	D13Mit283	D13Mit35	D13Mit48	D13Mit69
Chromosome 14(3)									
	D14Mit2	D14Mit95	D14Nds5						
Chromosome 15(5)									
	D15Mit234	D15Mit29	D15Mit34	D15Mit6	D15Mit90				
Chromosome 16 (7)									
	D16Mit110	D16Mit13	D16Mit211	D16Mit5	D16Mit57	D16Mit88	D16Mit94		
Chromosome 17 (11)									
	D17Mit11	D17Mit119	D17Mit152	D17Mit155	D17Mit176	D17Mit21	D17Mit221	D17Mit266	D17Mit51
	D17Mit52	D17Mit96							
Chromosome 18 (3)									
	D18Mit3	D18Mit40	D18Mit60						
Chromosome 19 (7)									
	D19Mit10	D19Mit10	D19Mit128	D19Mit18	D19Mit8	D19Mit85	D19Mit90		
Chromosome X (25)									
	DXMit119	DXMit121	DXMit143	DXMit149	DXMit154	DXMit156	DXMit16	DXMit189	DXMit197
	DXMit199	DXMit236	DXMit248	DXMit249	DXMit31	DXMit5	DXMit54	DXMit55	DXMit64
	DXMit67	DXMit73	DXMit74	DXMit84	DXMit89	DXMit95	DXMit99		

Fig. 1. A list of markers examined difference between C3H and CBA mouse in a total 256 markers.

parametric statistical analysis for establishing genetic linkage. Contingency tables consisting of affected and non-affected C3H/C3H and C3H/CBA strains were constructed, and chi square (χ^2) tests were performed with one degree of freedom. As recommended by Lander and Kruglyak, $P<0.0034$ ($\chi^2>8.58$) were the thresholds for suggestive linkage (10).

Production of inflammatory cytokines after exposure to CADS. To clarify the inflammatory cytokine response against CADS, we also examined the sequential change of serum cytokines after intraperitoneal injection of CADS. Twenty milligrams of CADS suspended in 0.2 ml of PBS(−) was injected intraperitoneally to C3H/HeN. Sera were obtained from sacrificed mice at each time ($N=5$) for 14 days after injection of CADS and then frozen at −80 C. Serum cytokines, such as interleukins IL-1β, IL-4, IL-6, IL-12, TNF-α, and IFN-γ were measured by using ELISA assay kits: IL-1β, IL-4, IL-6, IL-12, and TNF-α (Genzyme, Mass., U.S.A.), and IFN-γ (Pierce ENDOGEN, Qld, Australia).

Results

Histological Observations of Arteritis

Table 1 shows the incidence of vasculitis in the coronary artery and/or the aortic root in (CBA/JN×C3H/HeN)F1, (C3H/HeN×CBA/JN)F1, and [(CBA/JN×C3H/HeN)×C3H/HeN]N1 was 0%, 16.7%, and 20.7% respectively, while that in C3H/HeN parents was 71.1% (27/38), but in CBA/JN absence (0%, 0/27). Most cases of vasculitis were observed in the aortic root and/or the coronary artery (Fig. 2). All layers of these vessels showed severe inflammation, which is defined as 'productive granulomatous inflammation, but fibrinoid necrosis was rarely determined.' Intima showed various degrees of fibrocellular thickening associated with the lumen of coronary artery became stenotic. In addition to the disruption of internal and external elastic laminas, smooth muscle cells in media deteriorated from severe inflammation. Furthermore, the destruction of the normal structure of the coronary artery in some cases caused aneurismal dilatation. However, neither thrombotic occlusion nor myocardial infarction was observed. Histological differences of arteritis between N1 and C3H/HeN was not elucidated. Arteritis in other visceral organs such as renal artery, testicular artery, and abdominal aorta were rarely detected.

Linkage Analysis with Chromosome Mapping

Two hundred and fifty-six microsatellite markers were tested to segregate loci by original parental strains (Fig. 1). However, most markers were the same sequence length polymorphism between C3H/NeN and CBA/JN. Only 48 markers were selected for the linkage analysis (Table 2). Genome-wide interval mapping analysis between coronary artery and genetic markers for the identification of susceptibility loci was performed by using χ^2 test as described in "Materials and Methods." The markers on the chromosome 1 showed the association even though possibility on other chromosome loci may exist. Two of 11 markers on chromosome 1, *D1Mit171* and *D1Mit245* around 20.2 cM revealed suggestive linkage with P value of 0.0019 (Table 3). The other markers on chromosome 1 did not indicate the association. Based on the suggestive level of *D1Mit171* and *D1Mit245*, this region is thought to influence to the development of coronary arteritis. On the other chromosomes, the marker, *D4Mit285*, showed low probability of 0.017, but was not in the scope to designate an association.

Table 1. Affected rate of coronary arteritis after 9 weeks challenge with CADS

Mice	Affected rate (%)
C3H/HeN	71.1 (27/38)
CBA/JN	0 (0/27)
(C3H male×CBA female) F1	0 (0/9)
(C3H female×CBA male) F1	16.7 (1/6)
(CBA female×C3H male) F1×C3H	20.7 (24/115)

CBA/JN and C3H/HeN (CBA/JN×C3H/HeN) and N1 backcross progeny between F1 and C3H/HeN [(CBA/JN×C3H/HeN)×C3H/HeN] were prepared.

Circulation of Inflammatory Cytokines after Exposure to CADS

Sequential changes of inflammatory cytokines IL-12, IL-1β, TNF-α, IL-6, IFN-γ, and IL-4 in serum for 14 days after intraperitoneal injection of CADS were measured by ELISA assay. Both IL-1β and IL-12 levels in serum increased at 1 hr after injection of CADS, and then decreased gradually, but IL-12 did not decrease like profile of IL-1β (Fig. 3a). After increases of IL-1β and IL-12, levels of TNF-α and IL-6 peaked at 3 hr after the injection, and then restored to baseline by 24 hr (Fig. 3b). Levels of IFN-γ gradually increased over the same period, but no change in IL-4 level was noted (Fig. 3c).

Discussion

Some infectious microorganisms have been implicated in the etiology of KD, though primary causes remain an enigma (6, 11, 16, 22). These candidates of etiology may act as initial trigger to induce arteritis. The spontaneous arteritis model may not be well suited for study-

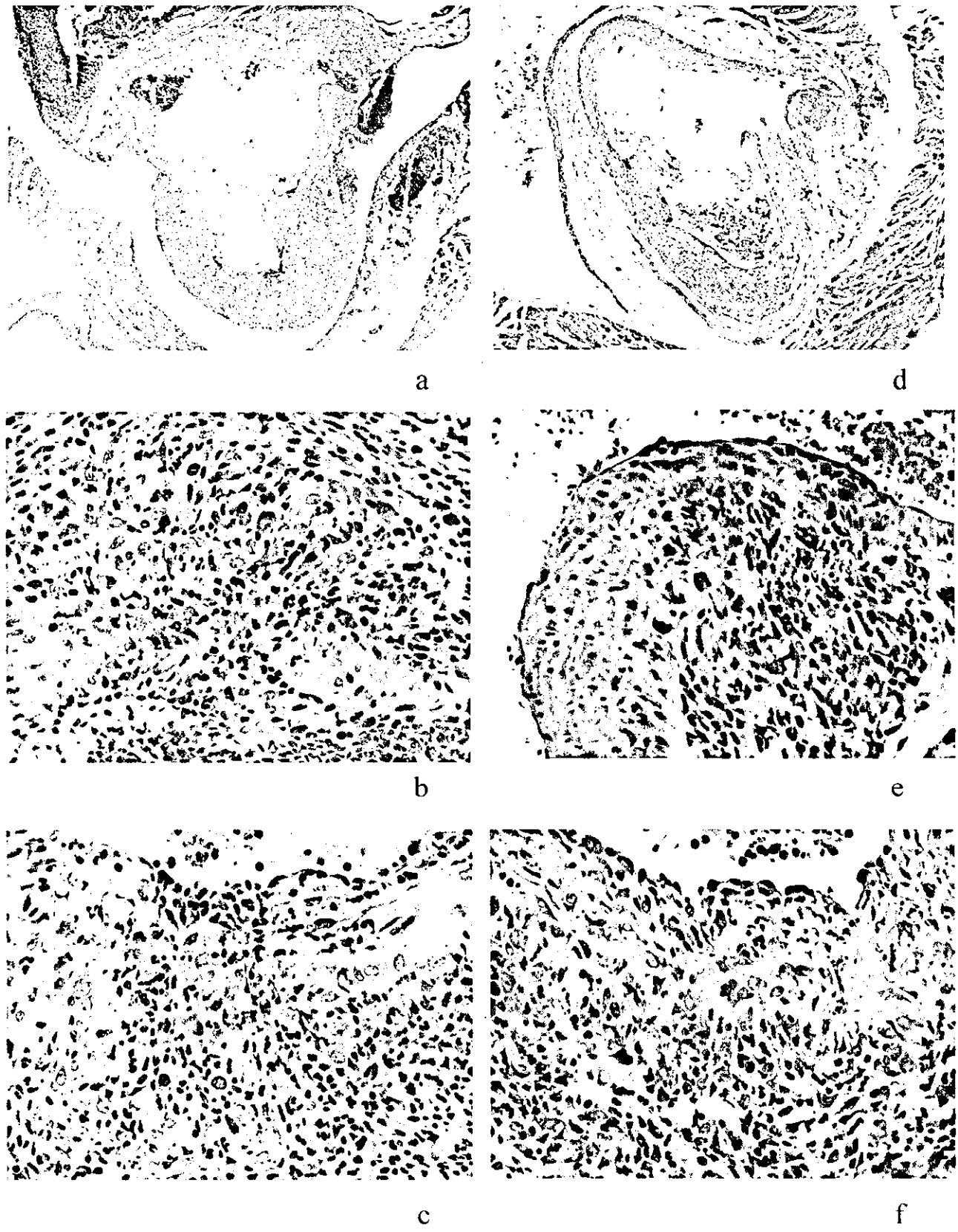

Fig. 2. Histological feature of coronary arteritis in N1 and C3H/HeN. (a) Vasculitis at the coronary artery and aortic root in N1 mouse (HE stain, ×40), (b) coronary arteritis in N1 mouse (HE stain, ×400), (c) aortitis in N1 mouse (HE stain, ×400), (d) coronary arteritis and aortitis in C3H/HeN (HE stain, ×40), (e) coronary arteritis in C3H/HeN (HE stain, ×400), (f) aortitis in C3H/HeN (HE stain, ×400).

Table 2. A list of the 48 markers used for the linkage analysis from 256 candidates for markers

Chromosome	Symbol	Position (cM)	Chromosome	Symbol	Position (cM)
1	D1Mit374	19.0	6	D6Mit345	46.0
1	D1Mit171	20.2	7	D7Mit232	26.8
1	D1Mit245	20.2	8	D8Mit224	17.0
1	D1Mit75	32.1	8	Mt2	45.0
1	D1Mit380	36.9	8	D8Mit14	67.0
1	D1Mit251	38.1	9	D9Mit2	17.0
1	D1Mcg3	38.9	9	Cyp1a2	31.0
1	D1Mcg6	39.9	9	D9Mit279	67.0
1	D1Mit7	41.0	10	D10Mit214	19.0
1	D1Mit200	80.0	11	Hoxb	56.0
1	Tgfbm2	106.3	12	D12Mit231	48.0
2	D2Mit92	41.4	13	D13Mit110	47.0
2	D2Mit206	51.4	14	D14Mit2	5.0
2	D2Mit311	83.1	14	Nfl	28.7
2	D2Mit456	86.3	15	D15Mit6	13.7
2	D2Mit265	105.0	16	D16Mit5	38.0
2	D2Mit200	107.0	17	D17Mit96	54.6
2	D2Mit457	108.0	18	D18Mit60	16.0
3	D3Mit90	4.6	19	D19Mit128	10.9
3	D3Mit200	77.3	19	D19Mit10	47.0
3	D3Mit323	84.9	X	DXMit74	20.0
4	D4Mit272	21.9	X	DXMit16	37.0
4	D4Mit285	71.0	X	DXMit121	67.0
4	D4Mit357	81.5			
5	D5Mit101	81.0			

Table 3. A list of markers that exhibited distribution disequilibrium from the 2×2 χ^2 based on a ratio of affected C3H/C3H:C3H/CBA to non-affected

Chromosome	Distance (cM)	Marker	Affected / Non-affected	χ^2	Probability
1	19.0	D1Mit374	18:6 / 34:45	7.52	0.0061
	20.2	D1Mit171	19:5 / 34:45	9.62	0.0019[a]
	20.2	D1Mit245	19:5 / 34:45	9.62	0.0019[a]
	32.1	D1Mit75	18:6 / 33:46	8.13	0.0044
	38.1	D1Mit251	17:7 / 30:49	8.01	0.0046
	38.9	D1Mcg3	15:9 / 31:48	4.03	0.0447
	39.9	D1Mcg6	15:9 / 31:48	4.03	0.0447
	41.0	D1Mit7	15:9 / 31:48	4.03	0.0447
4	71.0	D4Mit285	7:17 / 45:34	5.69	0.0171

[a] Suggestive linkage.

ing KD, because it requires an initial trigger from some infectious microorganisms to induce arteritis. On the other hand, our model requires injection of CADS to induce arteritis. This model is very useful for the study of the pathogenesis of arteritis in KD for two main reasons: 1) both the histological features and distribution of arteritis are similar to that of KD, and 2) infectious agents are required to induce the development of arteritis. The mechanisms of developing arteritis in patients with KD are still unclear; however, several reports have